

Estimating Mechanical Properties of the Left Ventricle Using Dynamic Modeling and Magnetic Resonance Imaging

Arye Nehorai, Aleksandar Jeremić

The University of Illinois at Chicago, Chicago, USA

Abstract

We present an algorithm for estimating active and passive mechanical properties of the left ventricle using magnetic resonance imaging (MRI) tissue-tagging and pressure measurements. We combine physical modeling with a finite-element formulation and dynamic analysis, and apply maximum likelihood to estimate the unknown parameters. We assume that the myocardium's stiffness tensor is anisotropic and non-homogeneous. Numerical examples demonstrate the applicability of our results.

1. Introduction

The estimation of the mechanical properties of the heart is important for validating constitutive models, detecting certain cardiac dysfunctions such as hypertrophy, and predicting heart failure [1]-[2]. Historically, material properties of the heart have been determined by *in vivo* pressure-volume studies employing simple mathematical models. This approach is useful for estimating global characteristics of the ventricles but is unsuitable for understanding the regional variations in the material properties or the anisotropy of the cardiac muscle. To fully characterize the complexities of the myocardial mechanical properties, an approach based on the theory of continuum mechanics is required. Recent advances in magnetic resonance imaging (MRI) and finite-element (FE) methods have enabled estimation of mechanical properties *in vivo* [3].

We present a method for determining the active and passive mechanical properties of the myocardium using 2D tagged MR images and pressure measurements. Our approach is based on dynamic analysis of large deformations [4]: we develop a 2D model to relate displacements of the tag points at various locations in the cross-sectional plane during the heart cycle to the mechanical parameters and ventricular pressure;

we then estimate these parameters by minimizing a distance measure between the predicted pressure and pressure measurements using the displacements measured from tagged MRI. We combine a finite-element formulation with dynamic modeling to determine the predicted pressure, followed by a maximum likelihood optimization of the distance measure. By exploiting the dynamics of the heart-wall's motion we should achieve improved estimation performance compared with existing quasi-static approaches, see e.g. [3].

2. Physical Modeling

The left ventricle (LV) is a complex mechanical system with respect to its geometry, structure, mechanical properties and processes that govern its motion.

We model the LV wall as an anisotropic, non-linear, non-homogeneous, hyper-elastic solid, [5]. A large number of existing ventricular models also assume incompressibility of the cardiac tissue, i.e. the volume does not change with stress. However, it has been shown that the intra-coronary blood volume varies in time [6], which makes the incompressibility assumption questionable in most models. Furthermore, in the case of 2D cross-sectional models the 2D incompressibility condition, i.e. constant cross-sectional area, is unrealistic since the cardiac through-plane motion is substantial, and hence incompressibility does not imply that the cross-sectional area remains constant. Therefore, we assume that cardiac tissue in the cross-sectional plane is compressible.

We use two coordinate systems in the governing equations. As a reference system we use a Cartesian coordinate system whose x, y plane lies in the cross-sectional plane of the ventricle. The deformation of the left ventricle is described by a motion in which a point (x, y) in the undeformed cross-sectional plane s (at time 0) moves to (\bar{x}, \bar{y}) in the deformed plane \bar{s} (at time t). Following [7] we select the end of the diastole as reference time $t = 0$ at which the ventricle is undeformed. The second coordinate system is defined with

This work was supported by the Air Force Office of Scientific Research under Grant F49620-97-1-0481, the National Science Foundation under Grant MIP-9615590 and the Office of Naval Research under Grant N00014-98-1-0542.

respect to the muscle fibers. These fibers are arranged in the continuum of helical layers and run parallel in each of them [8]. Thus, the material coordinate system is chosen as follows: the fiber axis x' lies in the layer and points in the fiber direction, the cross-fiber axis y' is the in-plane axis perpendicular to x' , and the transmural axis z' forms the right coordinate system i.e. $z' = x' \times y'$.

We split the ventricular stress vector $\boldsymbol{\tau}(x, y, t)$ into two parts: passive stress $\boldsymbol{\tau}_p(x, y, t)$, resulting from the area change of the myocardial tissue, and active (contractile) stress $\boldsymbol{\tau}_a(x, y, t)$ resulting from the isometric contraction of the muscle fiber. The passive stress vector is related to the potential function $w(x, y)$ (strain energy per unit volume)

$$\begin{aligned} \boldsymbol{\tau}_p &= \frac{\partial w(x, y)}{\partial \boldsymbol{\epsilon}}, \\ w(x, y) &= a \{ \exp [\boldsymbol{\epsilon}^T D(x, y) \boldsymbol{\epsilon}] - 1 \}, \end{aligned} \quad (1)$$

where a is the initial normal stiffness, $\boldsymbol{\epsilon}$ is a vector of strains, and $D(x, y)$ is the non-homogeneous myocardium stiffness matrix.

To model the non-homogeneity we propose to use a linear combination of an *a priori* known set of basis functions with unknown coefficients. Then, the (i, j) th entry of $D(x, y)$ is given by

$$D_{ij}(x, y) = \sum_k^{n_b} c_{ij}^k \phi_{ij}^k(x, y), \quad (2)$$

where $\{\phi_{ij}^k(x, y)\}$ is the set of basis functions, n_b is the number of functions, and c_{ij}^k the coefficients.

Note that in our model the non-homogeneity corresponds to the myocardium stiffness whereas the myocardium density ρ is assumed to be uniform. However, non-homogeneous density can be modeled similarly to the myocardium stiffness, with an appropriate set of basis functions.

The active stress model is adopted from [9]. Accordingly

$$\tau_f(t) = \tau_{\max} [1 - \cos\omega(t)]. \quad (3)$$

where $\tau_f(t)$ is the magnitude of the active stress in the fiber coordinate system, τ_{\max} the maximum isometric tension value, and

$$\omega(t) = \begin{cases} \frac{\pi}{t_0} t & t_d < t < t_0 \\ \frac{\pi}{t_r} \frac{t - t_0 + t_r}{t_r} & t_0 \leq t < t_0 + t_r \\ 0 & t_0 + t_r \leq t \end{cases}, \quad (4)$$

where t_d is the duration of the diastole, t_0 the time to peak-tension, and t_r is the duration of relaxation. The active stress $\boldsymbol{\tau}_a$ in the cross-sectional plane consists of two longitudinal components, $\tau_{a,x}$ and $\tau_{a,y}$, as

well as shear stress $\tau_{a,xy}$. The cross-sectional active stress is computed from $\tau_f(t)$ by applying a transformation [10] from the fiber coordinate system to the reference coordinate system. This transformation is a function of the fiber elevation and azimuth angles. Because both angles change smoothly from epicardium to endocardium, the cross-sectional active stress is non-homogeneous and can be approximated, similarly to the myocardium stiffness, using a different set of basis functions.

3. Finite-Element Approximation

The LV motion is determined by Navier-Stocks differential equation and a particular set of boundary conditions. In addition to the non-linear and non-homogeneous mechanical properties, the domain of interest (LV) is irregularly shaped. It has been proposed [11] that the finite-element (FE) method might be used for solving the inverse boundary problem.

We model the LV motion using the virtual displacements principle combined with a total Lagrangian formulation for large deformation dynamic analysis, and deformation-dependent loading, following [4]. The principle of virtual displacements requires that the work of external forces of the ventricle is equal to the virtual strain energy of internal stresses caused by arbitrary virtual displacements. Thus,

$$\begin{aligned} \int_{\bar{s}} \delta \boldsymbol{\epsilon}^T \boldsymbol{\tau} d\bar{s} &= \int_{\bar{l}_{en}} \delta \boldsymbol{u}^T \boldsymbol{n}_{en} p d\bar{l} - \rho \int_{\bar{s}} \delta \boldsymbol{u}^T \ddot{\boldsymbol{u}} d\bar{s} + \\ &- g \int_{\bar{l}_{ep}} \delta \boldsymbol{u}^T \boldsymbol{n}_{ep} (\boldsymbol{u}^T \boldsymbol{n}_{ep}) d\bar{l}, \end{aligned} \quad (5)$$

where \bar{s} is the deformed ventricle surface, $\delta \boldsymbol{\epsilon}$ is the virtual strain, \bar{l}_{en} and \bar{l}_{ep} are the endocardial and outer boundaries of the deformed ventricle, \boldsymbol{n}_{en} and \boldsymbol{n}_{ep} are unit vectors normal to the endocardial and outer boundaries pointing outside, g is the linear spring constant [3], $\delta \boldsymbol{u}$ is the virtual displacement, p is the ventricular pressure, and $\ddot{\boldsymbol{u}}$ is the second-order derivative of displacement function \boldsymbol{u} with respect to time. All variables in (5) are functions of x, y , and t except the pressure which is a function of time only. The l.h.s. of equation (5) corresponds to the virtual strain energy due to internal stresses. The first integral on the r.h.s. corresponds to the external work of boundary forces caused by ventricular pressure, the second integral to the effect of inertial forces (D'Alembert's principle), and the third integral to the effect of pericardial pressure.

We derive a finite-element formulation for (5) following [4]. The integration of (5) corresponds to all elements, but assembling contributions from all elements

is relatively straightforward. Thus, we will henceforth view (5) as involving integration over a single element.

We construct the FE mesh using the tag points as nodes. We approximate the epicardium and LV using a Fourier series representation of tag points located on these boundaries. As a result, the curved boundary segments and element shape functions can be represented by the linear blending method presented in [12, pp. 107-112].

Equation (5) determines the relation between the ventricular pressure and myocardial strain which is not directly available from the tagged MRI images. Hence, we need to relate the strain to the displacements of the tag points (FE mesh nodes) which can be measured directly. For this purpose, we use the displacement assumption [4] stating that within any given element $\mathbf{u}^e(x, y, t) = R^e(\bar{x}, \bar{y}, t)A^e(\bar{x}, \bar{y}, t)\mathbf{d}^e$, where \mathbf{d}^e is the nodal displacement vector, $R^e(\bar{x}, \bar{y}, t)$ is a matrix that transforms the generalized displacements to displacements at a point within the element, and $A^e(\bar{x}, \bar{y}, t)$ is the transformation matrix from the the nodal point displacements to the generalized displacements.

Finally, to compute the r.h.s. of (5), we use “equivalent forces” [4]. The boundary force at time t , i.e. $p(t)\mathbf{n}(x, y, t)$, can be referred to the undeformed configuration through

$$p(t)d\bar{l}(x, y, t) = p(t) \left| \frac{\partial \bar{x}}{\partial x} \right| \frac{\partial x}{\partial \bar{x}} dl(x, y, 0), \quad (6)$$

where $|\cdot|$ denotes determinant. The inertial force is computed similarly to the pressure generated force using $d\bar{s} = |\partial \bar{x} / \partial x| ds$. To compute $\partial x / \partial \bar{x}$ and $\partial \bar{x} / \partial x$ we use a surface interpolation technique [13] that employs surface polynomials for mapping between undeformed and deformed regions of the ventricle.

The FE formulation for a single element at time t is then given by

$$\rho M^e \ddot{\mathbf{d}}^e + (K_p^e + K_a^e) \mathbf{d}^e(t) + g \mathbf{b}^e = \mathbf{s}^e(\mathbf{d}(t)) p(t), \quad (7)$$

where M^e is the element mass matrix, K_p^e is the element passive stiffness matrix, K_a^e is the element active stiffness matrix, \mathbf{b}^e is the vector corresponding to the third integral on the r.h.s. of (5), and \mathbf{s}^e is the load vector corresponding to the first integral on . Since the contraction of the heart muscle is limited in duration the elements of K_a^e become 0 for $t > t_0 + t_r$.

Procedures for computing the stiffness mass matrices are given in [4] and expressions for the matrix entries are given in [14]. The global equation is derived using standard assembly procedures and is of the same form as (7) except that the structural matrices are referred to the global reference frame.

4. Parameter Estimation

We wish to estimate the unknown active and passive mechanical properties of the left ventricle. The active mechanical properties (parameters), denoted by $\boldsymbol{\theta}_a$, are the coefficients of the basis functions used for modeling the active stress. The passive mechanical properties $\boldsymbol{\theta}_p$ are the coefficients of the basis functions from equation (2) used for modeling the myocardial stiffness.

4.1. Statistical Model

The accuracy of the model (7) is limited by measurement and modeling errors. Modeling errors are due to inaccuracy of the FE approximation and physical modeling. We use the following assumptions: the MR images are taken at time points $\{t_m = m\Delta t, 1 \leq m \leq n\}$ where Δt is the time interval between two consecutive images, the nodal displacement vectors $\mathbf{d}_m = \mathbf{d}(t_m)$ are measured exactly from each image, and the ventricular pressure $p_m = p(t_m)$ is measured during each image acquisition. Introduce $\mathbf{s} = [\mathbf{s}_1^T, \dots, \mathbf{s}_n^T]^T$ and $\mathbf{b} = [\mathbf{b}_1^T, \dots, \mathbf{b}_n^T]^T$, which are the global vectors assembled from (7). Then lump the nodal displacement vectors into one vector $\mathbf{d} = [\mathbf{d}_1^T, \dots, \mathbf{d}_n^T]^T$ and similarly $\mathbf{y} = [p_1 \mathbf{s}_1^T, \dots, p_n \mathbf{s}_n^T]^T$.

Using a discrete second-order derivative, our statistical model is given by

$$\begin{aligned} \mathbf{y} &= A(\boldsymbol{\theta})\mathbf{d} + B\mathbf{v} + \mathbf{e}, \\ A(\boldsymbol{\theta}) &= K_p(\boldsymbol{\theta}_p) + K_a(\boldsymbol{\theta}_a), \\ B &= [MT\mathbf{d}\mathbf{b}], \end{aligned} \quad (8)$$

where T is a Toeplitz matrix with the (i, j) th entry $-2/\Delta t^2$ when $i = j$, $1/\Delta t^2$ when $|i - j| = 1$, and 0 elsewhere, and $\mathbf{v} = [\rho g]^T$. Also, $\boldsymbol{\theta} = [\boldsymbol{\theta}_a^T, \boldsymbol{\theta}_p^T]^T$, and \mathbf{e} is the residual error (noise). We assume that the error is zero-mean Gaussian distributed with covariance $\Sigma = \sigma^2 I$, where σ^2 is the unknown variance. Therefore, the vector of unknown parameters is $[\boldsymbol{\theta}_a^T, \boldsymbol{\theta}_p^T, \rho, \sigma^2]^T$.

4.2. Estimation Algorithm

To estimate the unknown parameters we use the maximum likelihood (ML) estimator. The likelihood function is

$$l(\mathbf{y}) = (2\pi\sigma^2)^{-n/2} \exp \left\{ -\frac{1}{2\sigma^2} \|\mathbf{y} - A(\boldsymbol{\theta})\mathbf{d} - B\mathbf{v}\|^2 \right\}. \quad (9)$$

The ML estimate of the unknown parameters [15] is then given by

$$\boldsymbol{\theta} = \operatorname{argmin} \left\{ \|\mathbf{y} - A(\boldsymbol{\theta})\mathbf{d} - B\mathbf{v}\|^2 \right\},$$

$$\begin{aligned}\hat{\mathbf{v}} &= (B^T B)^{-1} B^T (\mathbf{y} - A(\hat{\boldsymbol{\theta}}) \mathbf{d}), \\ \hat{\sigma}^2 &= \frac{1}{n} \|\mathbf{y} - A(\hat{\boldsymbol{\theta}}) \mathbf{d} - B \hat{\mathbf{v}}\|^2,\end{aligned}\quad (10)$$

where $B = [M^T \mathbf{d} \mathbf{b}]$ and $\mathbf{v} = [\rho \ g]^T$.

If the number of unknown parameters is large we can use a two-stage estimation procedure in which $[\boldsymbol{\theta}_p^T, \rho, \sigma^2]$ are first estimated, independently of $\boldsymbol{\theta}_a$. In the second stage, we consider these parameters as known and estimate $\boldsymbol{\theta}_a$. This technique is sub-optimal and hence should be used only if necessary, for example when the joint model is not identifiable.

5. Numerical Examples

We present numerical examples to demonstrate the applicability of the proposed algorithms. The measurements are obtained by simulating the LV motion using the forward model from Sections 2 and 3. We use $\{1, x, y, xy, x^2, y^2\}$ as basis functions for the stiffness matrix and $\{1, \cos x, \cos y, \sin x, \sin y, \cos(xy), \sin(xy)\}$ for generating the active stress. We select the basis functions for the active stress as appropriate for modeling cross-sectional variations of active stress due to changes in the fiber elevation and azimuth angles. We select the basis-function coefficients so that the average values of the stiffness matrix entries and active stress are the same as in [3] and [9] respectively. The time-dependent activation model, $t_0 = 0.1\text{s}$ and $t_r = 0.4\text{s}$ is adopted from [9]. The heart periodic rate is set to $t_c = 0.83\text{s}$ corresponding to 72 beats per minute. The pressure measurements are taken from [3]. The time increment Δt was set to 0.02s. To account for the errors discussed in Section 4.1 we add Gaussian noise to the pressure measurements. We define the signal-to-noise ratio (SNR) as the ratio of signal (pressure measurements) power to noise variance. We test the performance of the algorithm for SNR= 10dB and 0dB. As a performance measure we use the normalized root mean square error r. m. s. = $\|\hat{\boldsymbol{\theta}} - \boldsymbol{\theta}\|/\|\boldsymbol{\theta}\|$.

In Figs. 1 and 2 we present the true and estimated value of $D_{11}(x, y)$ for SNR= 0dB. The r. m. s. errors, calculated for all parameters, are: 0.07 for SNR= 10dB and 0.11 for SNR= 0dB.

6. References

- [1] Soufer R. *et al*, *Am. J. Cardiol.*, vol. 55, pp. 1032-1036, 1985.
- [2] Hess O. *et al*, *Circ. Res.*, vol. 52, pp. 387-400, 1983.
- [3] Moulton M. J. *et al*, *Int. J. Cardiac Imaging*, vol. 12, pp. 153-167, Dec. 1996.
- [4] Bathe K. *et al*, in *Int. J. Num. Met. Eng.*, vol. 9, pp. 353-386, Sep. 1975.

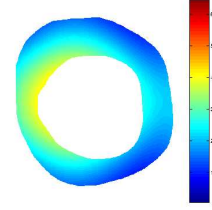


Figure 1: Actual myocardial elastic modulus $D_{11}(x, y)$.

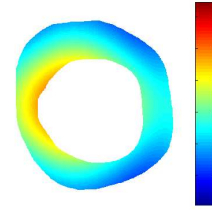


Figure 2: Estimated myocardial elastic modulus $\hat{D}_{11}(x, y)$, SNR= 10dB.

- [5] Fung Y. C., "Biomechanics," Springer-Verlag, New York, 1987.
- [6] Spaan J. A. E., *Circ. Res.*, vol. 56, pp. 293-309, 1985.
- [7] Redaelli A. *et al*, *Meccanica*, vol. 32, pp. 53-70, 1997.
- [8] Streeter Jr. D. D. *et al*, in J. Baan, A. Noordergraaf, and J. Raines (eds), *Cardiovascular System Dynamics*, pp. 73-84, MIT Press, Cambridge, MA, 1978.
- [9] Guccione J. M. *et al*, *ASME J. Biomech. Engng.*, vol. 115, pp. 82-90, 1993.
- [10] Biot M. A., *Mechanics of Incremental Deformations*, John Wiley & Sons, New York, 1948.
- [11] Yin F.C., "Biomechanics," Springer-Verlag, New York, 1987.
- [12] Szabo B., and Babuska I., *Finite Element Analysis*, John Wiley & Sons New York, 1991.
- [13] Moulton M. J. *et al*, *Am. J. Physiol.*, vol. 270, pp. H:281-297, Jan. 1996.
- [14] Nehorai A. *et al*, full version of this paper *in preparation*.
- [15] Stoica P. *et al*, *IEEE Trans. Acoust. Speech, Signal Processing*, vol. 37, pp. 720-741, May 1989.

Arye Nehorai
The University of Illinois at Chicago
EECS Department (M/C 154)
851 S Morgan St.
Chicago, IL, 60607
USA
e-mail: nehorai@eecs.uic.edu